

SUPPLEMENTAL INFORMATION

PRC2 is required to maintain expression of the maternal *Gtl2-Rian-Mirg* locus by preventing *de novo* DNA methylation in mouse embryonic stem cells

Partha Pratim Das, David A. Hendrix, Effie Apostolou, Alice H. Buchner, Matthew C. Canver, Semir Beyaz, Damir Ljuboja, Rachael Kuintzle, Woojin Kim, Rahul Karnik, Zhen Shao, Huafeng Xie, Jian Xu, Alejandro De Los Angeles, Yingying Zhang, Junho Choe, Don Leong Jia Jun, Xiaohua Shen, Richard I. Gregory, George Q. Daley, Alexander Meissner, Manolis Kellis, Konrad Hochedlinger, Jonghwan Kim, Stuart H. Orkin

SUPPLEMENTAL DATA

Supplemental figures and legends

Figure S1

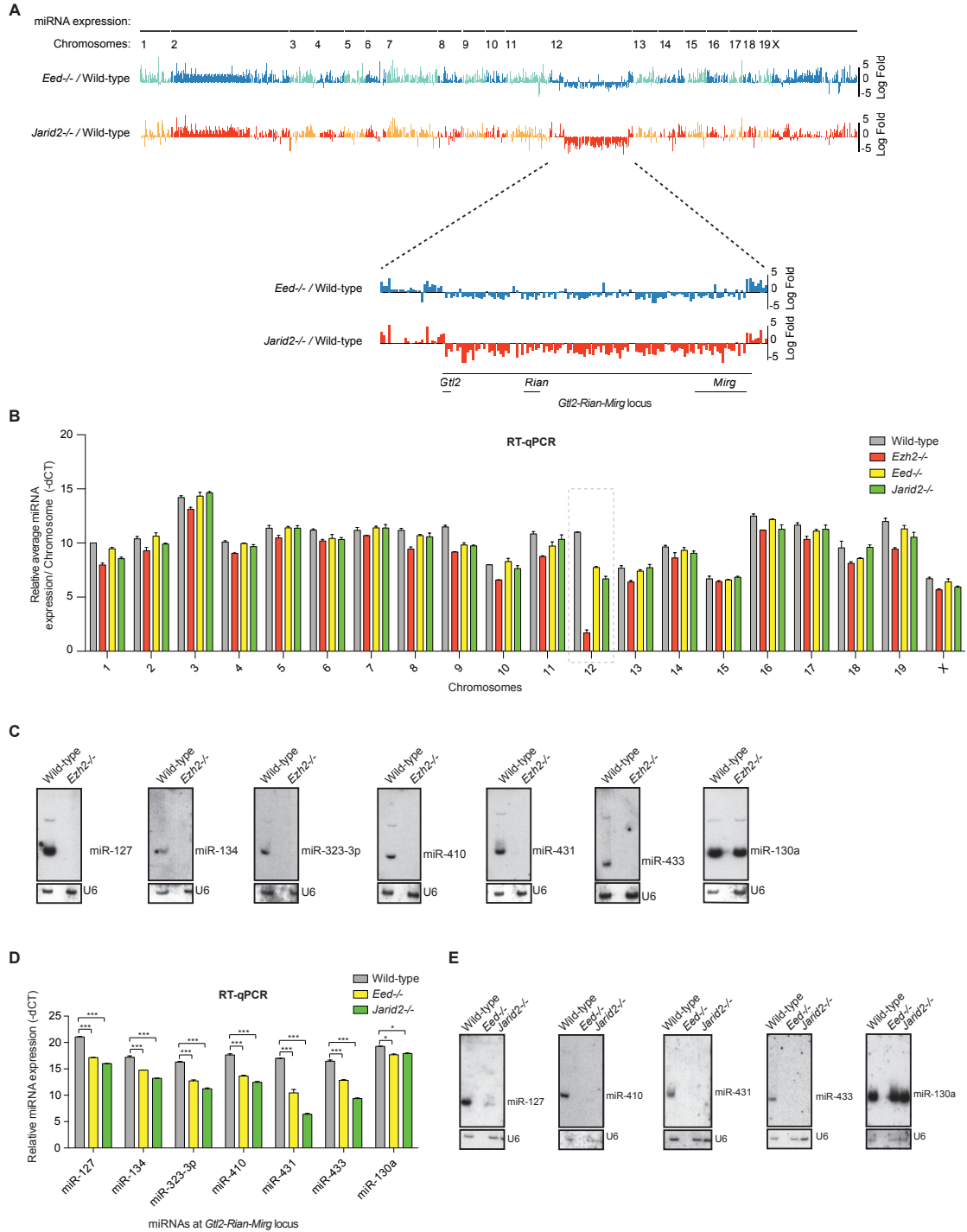


Figure S1. PRC2 is required to maintain expression of maternal miRNAs and lncRNAs at the *Gtl2-Rian-Mirg* locus (related to Figure 1)

(A) Small RNA-seq demonstrates log-fold change of miRNA expression in *Eed*^{-/-} and *Jarid2*^{-/-} mESCs as compared to wild-type. Significantly reduced expression of a cluster of miRNAs is observed at the *Gtl2-Rian-Mirg* locus of chromosome 12 in *Eed*^{-/-} and *Jarid2*^{-/-} mESCs.

(B) RT-qPCR analysis of miRNA expression per chromosome shows significant reduction of the miRNAs expression from chromosome 12 in *Ezh2*^{-/-}, *Eed*^{-/-} and *Jarid2*^{-/-} mESCs. Data are represented as mean +/- SEM (n=2); p-values were calculated using a 2way ANOVA; ***p <0.0001.

(C) Northern-blot confirms dramatically reduced expression of maternal miRNAs from the *Gtl2-Rian-Mirg* locus in *Ezh2*^{-/-} mESCs. miR-130a is shown as a control.

(D-E) RT-qPCR (D) and Northern-blot (E) confirm significantly reduced expression of maternal miRNAs from the *Gtl2-Rian-Mirg* locus in *Eed*^{-/-} and *Jarid2*^{-/-} mESCs. miR-130a is shown as a control. For RT-qPCR, miRNA expression data are represented as mean +/- SEM (n=3); p-values were calculated using a 2 way ANOVA; ***p <0.0001, *p <0.01.

(F) No significant changes in mRNA expression of *Dicer*, *Dgcr8*, and *Ago2* are observed in absence of *Ezh2*, *Eed* and *Jarid2* of PRC2. Transcript levels were normalized using *Gapdh*. mRNA expression data are represented as mean +/- SEM (n=3); p-values were calculated using a 2-way ANOVA; ns (non-significant). Protein levels of *Drosha* and *Ago2* were unaffected in wild-type and *Ezh2*^{-/-}. Actin is shown as a loading control for Western blot.

(G) RNA-seq reveals significant reduction of Gtl2, Rian and Mirg lncRNAs expression in absence of Ezh2, Eed and Jarid2.

(H) RT-qPCR shows dramatically reduced expression of maternal miRNAs from the *Gtl2-Rian-Mirg* locus in an independent *Ezh2*^{-/-} clone. miR-130a shown as a control. Data are represented as mean +/- SEM (n=3); p-values were calculated using a 2 way ANOVA; ***p <0.0001, ns (non-significant).

(I) RT-qPCR shows dramatic reduction of maternal Gtl2, Rian and Mirg lncRNA expression in an independent *Ezh2*^{-/-} clone as compared to wild-type. Transcript levels were normalized to Gapdh. Data are represented as mean +/- SEM (n=3); p-values were calculated using a 2 way ANOVA; ***p <0.0001, **p <0.001, *p <0.01 and ns (non-significant).

(J) RT-qPCR shows significant reduction of maternal Gtl2, Rian and Mirg lncRNAs expression in *Eed*^{-/-} and *Jarid2*^{-/-} mESCs as compared to wild-type. Transcript levels were normalized to Gapdh. Data are represented as mean +/- SEM (n=3); p-values were calculated using a 2 way ANOVA; ***p <0.0001, **p <0.001, *p <0.01 and ns (non-significant).

(K) mRNA expression (microarray) analysis of all imprinted genes shows differential expression of imprinted genes in the absence of components of PRC2. Most significant reduction was observed for Gtl2 and Rian, as well as for H19 expression, compared to other imprinted genes in the absence of PRC2 components. Reduced expression of Gtl2 and Rian was consistent in all PRC2 mutants, Ezh2, Eed and Jarid2; whereas H19 was down-regulated only in the absence of Ezh2 and Jarid2.

(L) RT-qPCR confirms reduced expression of H19 in the absence of Ezh2 and Jarid2,

same as microarray data. Three individual primer pairs of H19 yielded similar results. Data are represented as mean +/- SEM (n=3); p-values were calculated using a 2 way ANOVA; ***p <0.0001.

Figure S2

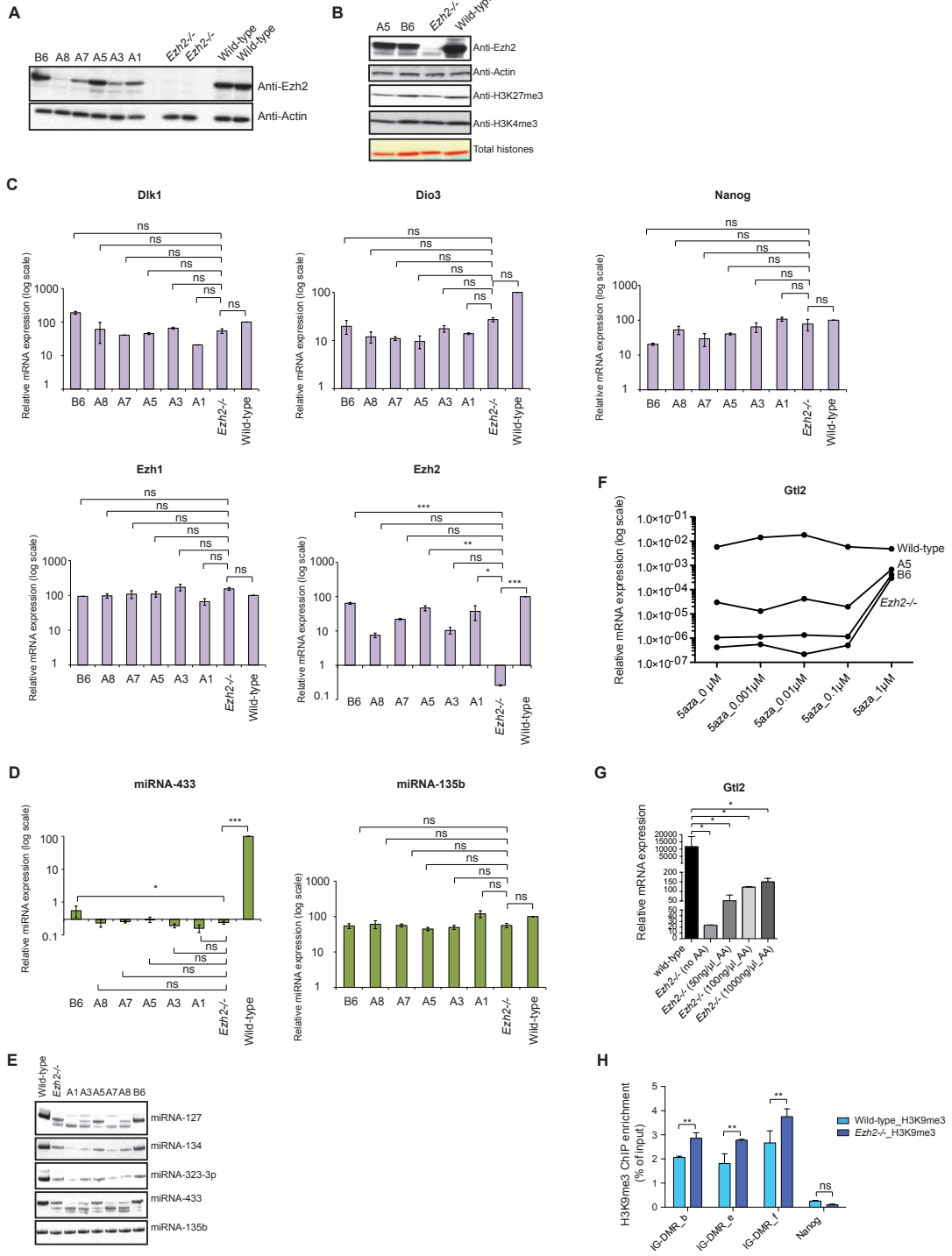


Figure S2. Methylation of the *Gtl2-Rian-Mirg* locus in the absence of PRC2 (related to Figure 2)

(A) Several individual Ezh2 rescue clones express different levels of exogenous Ezh2; A5 and B6 express near endogenous levels of Ezh2. Actin was used as a loading control.

(B) Ezh2 rescue clone (B6) restores global H3K27me3 similar to wild-type.

(C) RT-qPCR shows that reintroduction of Ezh2 in *Ezh2*^{-/-} mESCs has no significant effect on *Dlk1*, *Dio3* expression. Expression of *Nanog* and *Ezh1* was used as additional controls. Ezh2 expression shows different mRNA levels in different Ezh2 rescue clones. Data are represented as mean \pm SEM (n=3); p-values were calculated using one-way ANOVA; ***p < 0.0001, **P < 0.01, *p < 0.01, ns (non-significant).

(D) Ezh2 rescue clones, A5 and B6 that express near endogenous level of Ezh2 (Figures S2A and S2C), fail to restore the expression of maternal miRNAs from the *Gtl2-Rian-Mirg* locus (for example miR-433). miRNA expression is shown as mean \pm SEM (n=3); p-values were calculated using a one-way ANOVA; ***p < 0.0001, *p < 0.01, ns (non-significant). miR-135b was used as an internal control.

(E) Denaturing PAGE gel electrophoresis shows miRNA expression in Ezh2 rescue clones.

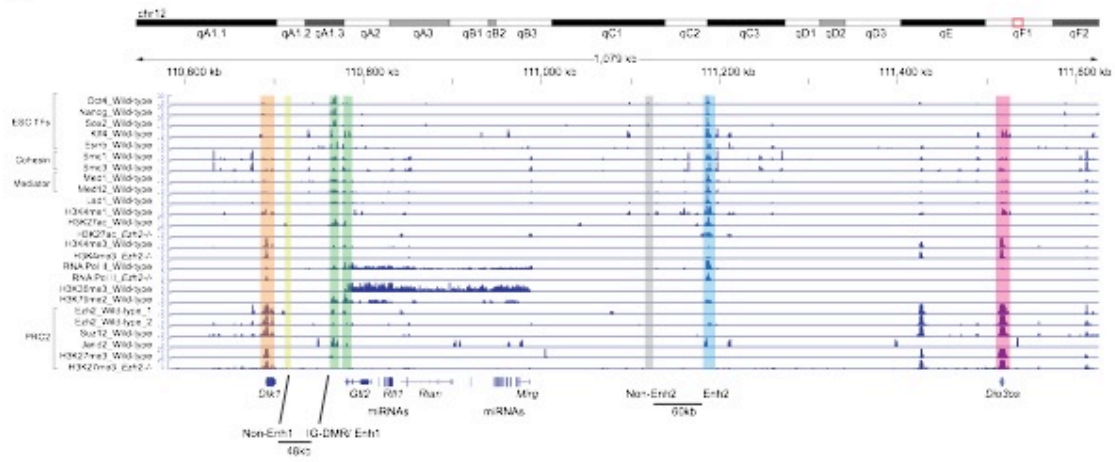
(F) Treatment with the Dnmt inhibitor, 5-azacitidine (5-aza) at high concentration (1 μ M) only partially restores *Gtl2* expression in *Ezh2*^{-/-} mESCs and Ezh2 rescue clones (A5 & B6).

(G) High concentration of ascorbic acid (vitamin C) treatment fails to restore *Gtl2* expression in *Ezh2*^{-/-} mESCs.

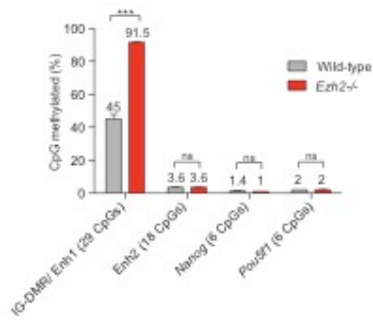
(H) ChIP-qPCR shows increased H3K9me3 occupancy at the IG-DMR locus in *Ezh2*^{-/-} mESCs compared to wild-type.

Figure S3

A



B



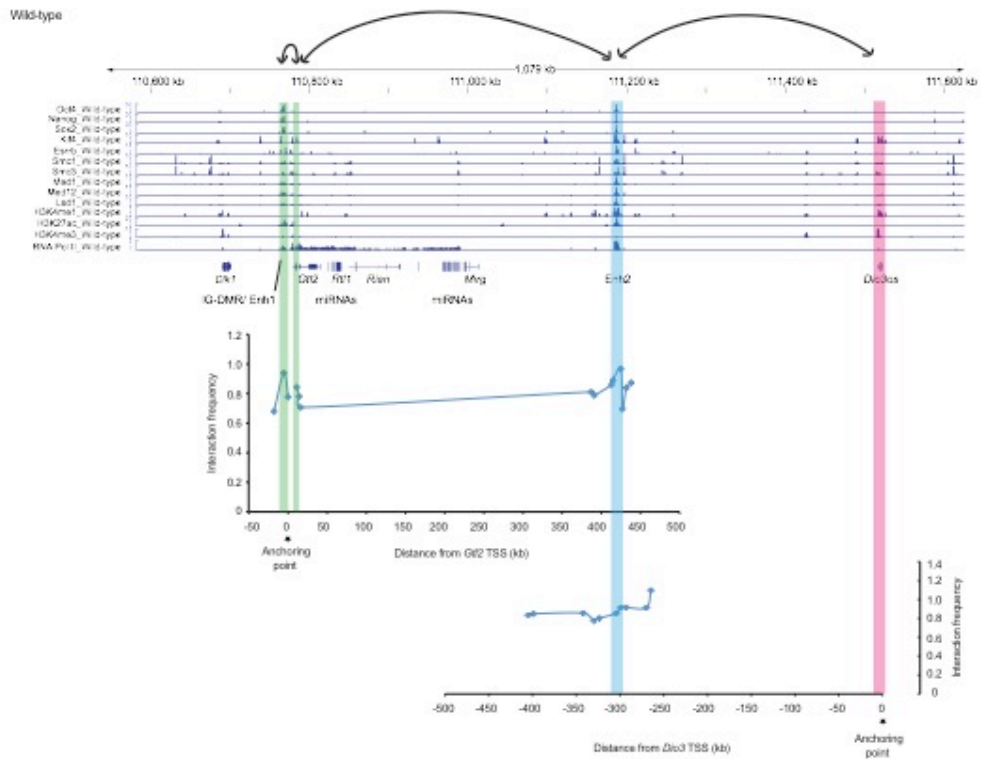
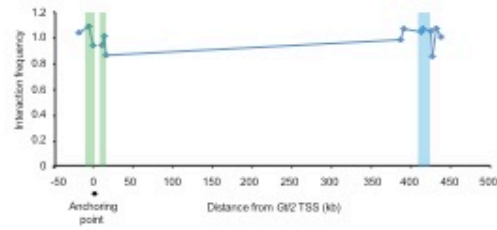
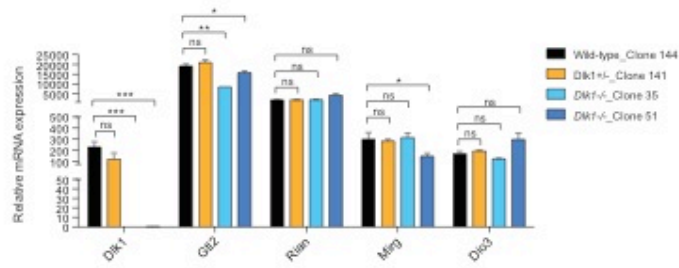
C*Ezh2^{-/-}***D**

Figure S3. IG-DMR/Enh1 serves as an enhancer for the *Gtl2-Rian-Mirg* locus (related to Figure 3)

(A) Genomic tracks display occupancy of factors and histone marks at the *Dlk1-Dio3* gene cluster. *Dlk1* promoter, *Dio3* promoter, *Gtl2* promoter, IG-DMR/Enh1, Enh2, Non-Enh1 and Non-Enh2 regions are highlighted.

(B) DNAm (%) was analyzed at IG-DMR/Enh1 and Enh2 in *Ezh2*^{-/-} mESCs as compared to wild-type. The Enh2 region is unmethylated. DNAm levels at the *Nanog* and *Oct4* proximal promoters were used as controls. Data are represented as mean +/- SEM (n=3); p-values were calculated using a 2 way ANOVA; ***p <0.0001, ns (non-significant).

(C) 3C demonstrates that both Enh1 and Enh2 loop into proximity with *Gtl2* promoter in *Ezh2* independent manner. No interaction was observed between Enh2 and the *Dio3* promoter.

(D) Biallelic deletion of the *Dlk1* promoter reveals no effect on the *Gtl2-Rian-Mirg* locus.

Figure S4

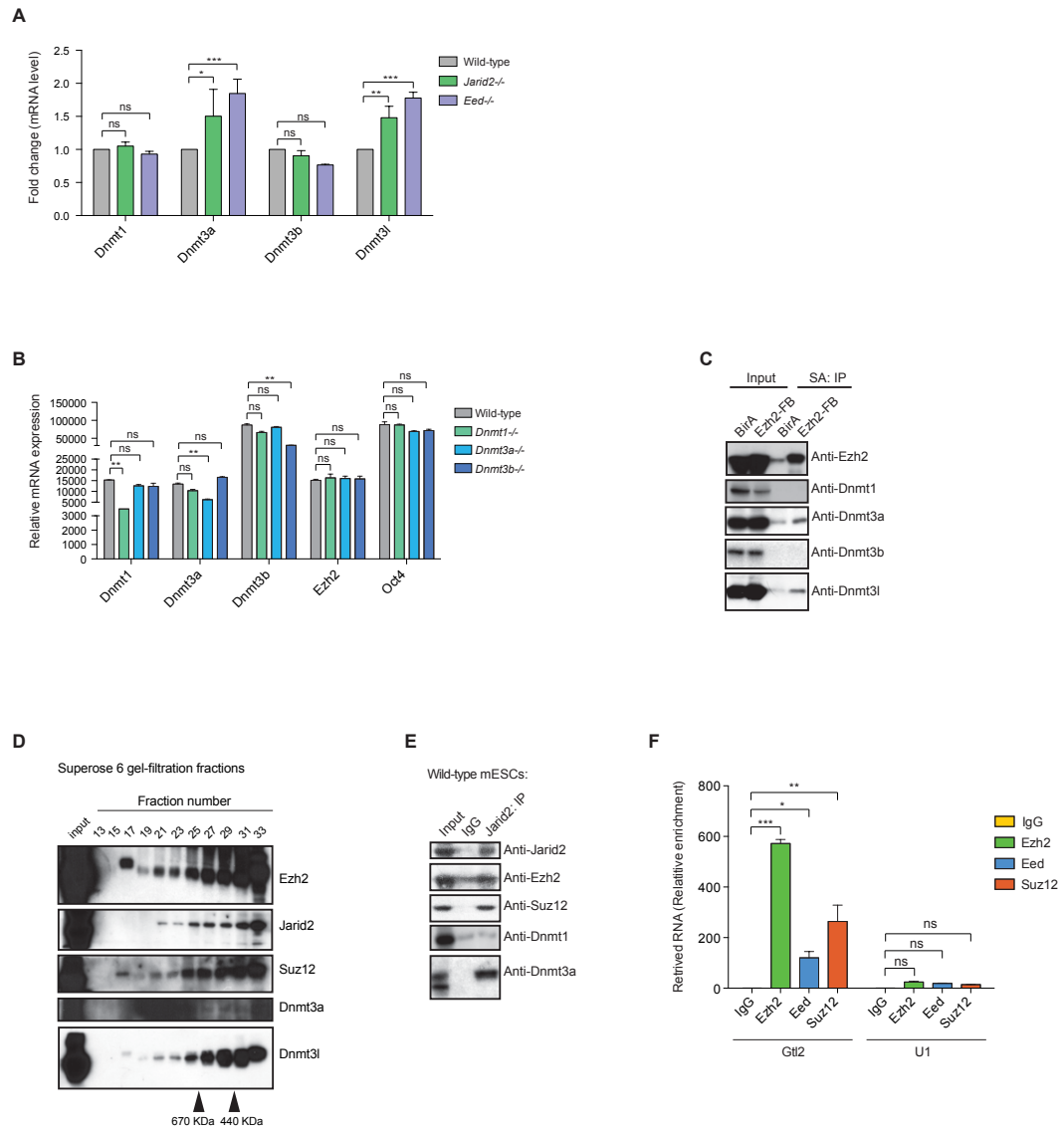


Figure S4. PRC2 physically interacts with Dnmt3a/3l (related to Figure 4)

(A) Expression of Dnmt3a and Dnmt3l is up-regulated in *Eed*^{-/-} and *Jarid2*^{-/-} mESCs compared to wild-type. Transcript levels were normalized to Gapdh. Data are represented as mean +/- SEM (n=3); p-values were calculated using a 2-way ANOVA; ***p <0.0001, **p <0.001, *p <0.01, ns (non-significant).

(B) mRNA expression of Ezh2 is unchanged in absence of Dnmts. Individual *Dnmt* knockout (KO) mESCs show significant down-regulation of the corresponding Dnmts. Transcript levels were normalized to Gapdh. Data are represented as mean +/- SEM (n=3); p-values were calculated using a 2-way ANOVA; **p <0.001, ns (non-significant).

(C) Flag-Biotin tagged-Ezh2 was immunoprecipitated from mESCs nuclear extract using streptavidin beads; specific interaction between Ezh2 and Dnmt3a/Dnmt3l was observed.

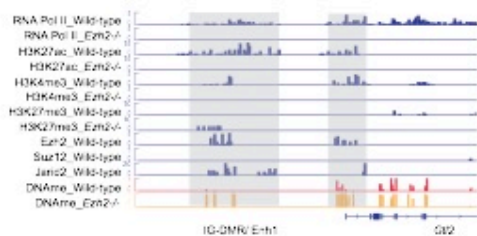
(D) Western blot analysis of Superose 6 gel-filtration fractions. Whole-cell lysates from mESCs were fractionated. Dnmt3a and Dnmt3l both were eluted in the same fractions as PRC2 components- Ezh2, Jarid2 and Suz12.

(E) Endogenous Jarid2 immunoprecipitated from mESCs nuclear extract shows specific interaction with components of PRC2 (Ezh2 and Suz12) and Dnmt3a.

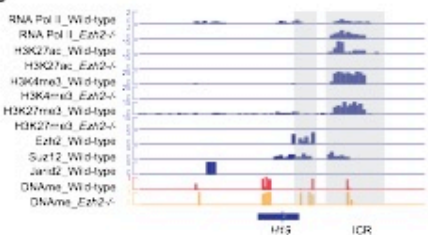
(F) RNA immunoprecipitation (RIP) demonstrates interaction of Gtl2 lncRNA with Ezh2, Eed and Suz12 of PRC2 complex. U1 RNA was used as control. Data are represented as mean +/- SEM (n=3); p-values were calculated using a 2-way ANOVA; ***p <0.0001, **p <0.001, *p <0.01, ns (non-significant).

Figure S5

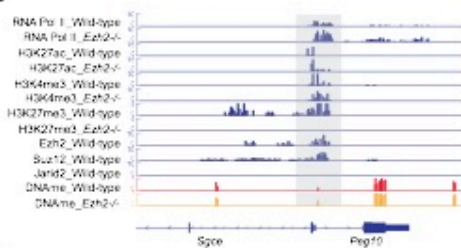
A



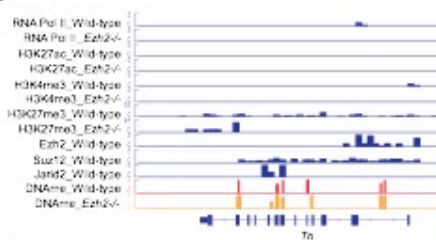
B



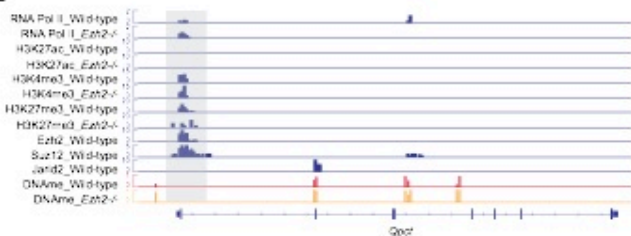
C



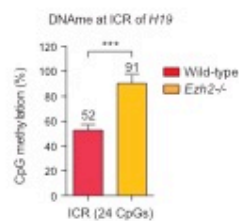
D



E



F



G

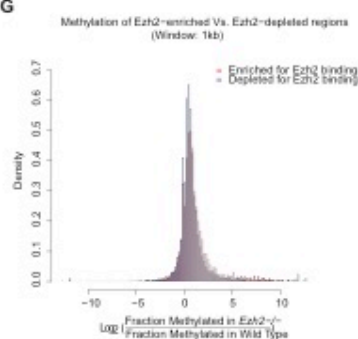


Figure S5. PRC2 antagonizes *de novo* DNAm at the IG-DMR through distinct mechanism (related to Figure 5)

(A-E) Genomic tracks display occupancy of histone marks, RNA Pol II, PRC2 (Ezh2, Suz12, Jarid2 and H3K27me3) and DNAm levels at selected down-regulated (*Gtl2*, *H19*, *Sgce* and *Peg10*), up-regulated (*Qpct*) and unchanged (*Th*) imprinted gene loci upon depletion of Ezh2/PRC2. Occupancy of H3K4me3 and H3K27ac is reduced at both the imprinting control regions- IG-DMR (for *Gtl2-Rian-Mir* locus) and ICR (for *H19*) in the absence of Ezh2 (A, B), and relates to the reduced expression of *Gtl2*, *Rian* and *H19*. PRC2/H3K27me3 occupies strongly at the ICR of *H19*, and ICR gains DNAm in absence of Ezh2/PRC2, whereas the IG-DMR weakly occupied by Ezh2/PRC2 and with no detectable H3K27me3 deposition, and gains DNAm (A, B). Two other down-regulated imprinted genes, *Sgce* and *Peg10*, are occupied with PRC2/H3K27me3, but fail to gain DNAm in absence of Ezh2/PRC2 (C). *Th*, an imprinted gene whose expression is unchanged in the absence of Ezh2/PRC2, does not reveal changes in factor binding, histone marks and DNAm (D). The up-regulated imprinted gene, *Qpct*, shows loss of H3K27me3 without gain of DNAm upon loss of Ezh2/PRC2 (E), indicating that PRC2 most probably regulates these imprinted gene loci in a different fashion, directly or indirectly.

(F) Analysis of 24 CpGs at the ICR of *H19* shows gain of DNAm (%) in *Ezh2*^{-/-} mESCs compared to wild-type. Data are represented as mean +/- SEM (n=3); p-values were calculated using a 2-way ANOVA; ***p < 0.0001.

(G) Regions of statistical enrichment and depletion for Ezh2 binding were determined by comparing Ezh2 ChIP-Seq to input reads with SICER using a window size of 1kb. For

each condition, the histogram compares the distributions of the log-fold change of the fraction of methylated dimers (in *Ezh2*^{-/-} compared to wild type) across all regions. *Ezh2*-enriched regions show enhanced methylation and these two distributions are different, as determined by a KS test, with a p-value less than 2.2e-16.

Figure S6

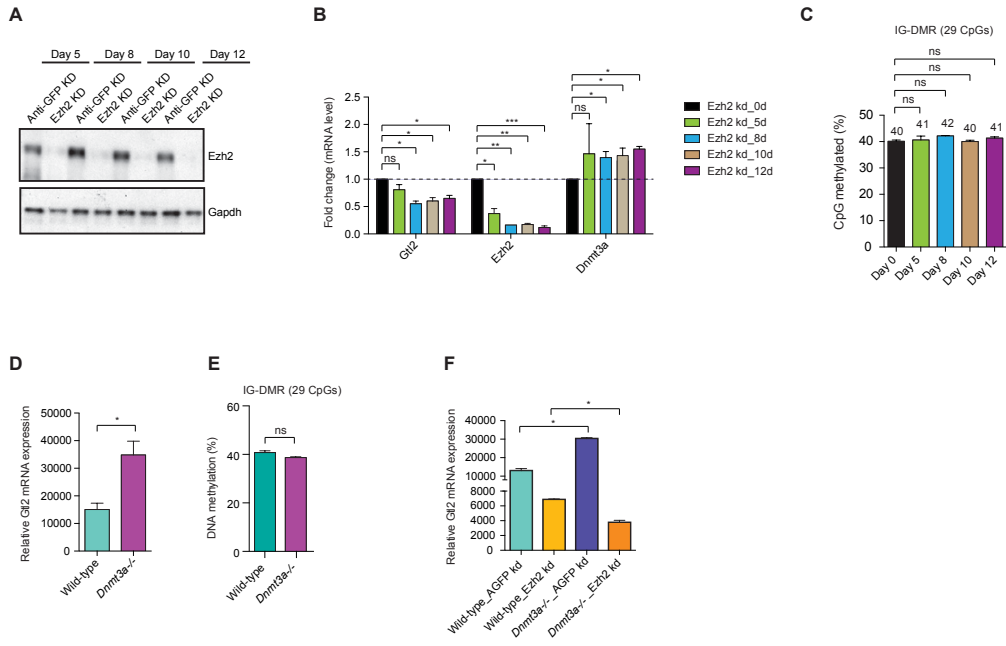


Figure S6. PRC2 protects IG-DMR from *de novo* DNAm to allow proper expression of the maternal *Gtl2-Rian-Mirg* locus (related to Figure 6)

(A) Time course experiment of knockdown of Ezh2, where Ezh2 protein level was significantly reduced. Gapdh used as an internal control.

(B) Knockdown of Ezh2 shows reduced expression of Gtl2 and increased expression of Dnmt3a. Transcript levels were normalized to Gapdh. Data are represented as mean +/- SEM (n=3); p-values were calculated using a 2-way ANOVA; ***p <0.0001, **p <0.001, *p <0.01 and ns (non-significant).

(C) Analysis of 29 CpGs at the IG-DMR shows no significant changes of DNAm (%) levels upon knockdown of Ezh2 at different time points. Data are represented as mean +/- SEM (n=3); p-values were calculated using a 2-way ANOVA; ns (non-significant).

(D) Deletion of *Dnmt3a* (*Dnmt3a*^{-/-}) shows mild increase of Gtl2 expression (RT-qPCR), but no significant change of DNAm level at the IG-DMR (E). Data are represented as mean +/- SEM (n=3); p-values were calculated using a 2-way ANOVA; *p <0.01, ns (non-significant).

(F) Depletion of Ezh2 in *Dnmt3a*^{-/-} mESCs show reduced Gtl2 expression (RT-qPCR). Data are represented as mean +/- SEM (n=3); p-values were calculated using a 2-way ANOVA; *p <0.01.

Figure S7

A

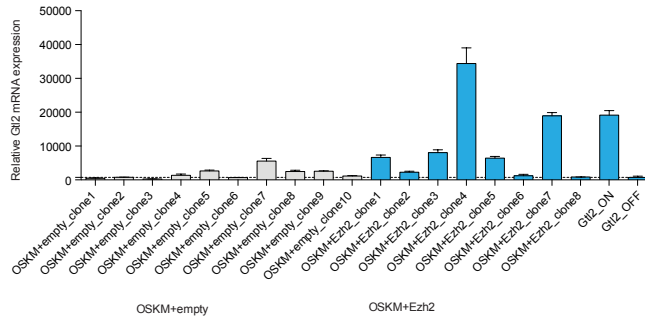


Figure S7. Overexpression of Ezh2 increases efficiency of “*Gtl2*^{ON} clones” during somatic cell reprogramming (related to Figure 7)

Overexpression of Ezh2 increases Gtl2 expression and efficiency of “*Gtl2*^{ON} clones” (1 iPSCs clone out of 10 iPSCs clones with OSKM+empty; and 5 iPSCs clones out of 8 iPSCs clones with OSKM+Ezh2, i.e increase efficiency of *Gtl2*^{ON} iPSCs clones up to ~50-60%) during somatic cell reprogramming.

Supplemental tables

Table S1.

High-throughput small RNA-Seq and RNA-seq data summary (related to Figure 1)

Sample names	Total reads sequenced	Total aligned to mm9
Wild-type_smRNASeq_R1	128345588	117065061
Wild-type_smRNASeq_R2	148608928	129251255
<i>Ezh2</i> ^{-/-} _smRNASeq_R1	130155426	115823634
<i>Ezh2</i> ^{-/-} _smRNASeq_R2	142044658	128072042
<i>Eed</i> ^{-/-} _smRNASeq_R1	124417057	114288285
<i>Eed</i> ^{-/-} _smRNASeq_R2	164454580	152960461
<i>Jarid2</i> ^{-/-} _smRNASeq_R1	68950485	62259756

Sample names	Total Sequenced Reads
Wild-type_RNASeq_R1	84740020
Wild-type_RNASeq_R2	151053542
<i>Ezh2</i> ^{-/-} _RNASeq_R1	93154862
<i>Ezh2</i> ^{-/-} _RNASeq_R2	137561873
<i>Eed</i> ^{-/-} _RNASeq_R1	37489298
<i>Eed</i> ^{-/-} _RNASeq_R2	110000921
<i>Jarid2</i> ^{-/-} _RNASeq_R1	56476890
<i>Jarid2</i> ^{-/-} _RNASeq_R2	140278885

Table S2. High-throughput ChIP-Seq data summary (related to Figure 3)

Sample names	Total Sequenced Reads
H3K4me3 wild-type	144281126
H3K4me3 <i>Ezh2</i> ^{-/-}	108742136
H3K27me3 wild-type	15793532
H3K27me3 <i>Ezh2</i> ^{-/-}	108098497
H3K27ac wild-type	128603319
H3K27ac <i>Ezh2</i> ^{-/-}	116156052
RNA Pol II wild-type	113379190
RNA Pol II <i>Ezh2</i> ^{-/-}	47463655
Wild-type input DNA_R1	50043014
Wild-type input DNA_R2	51639593
Wild-type input DNA_R3	44768252
<i>Ezh2</i> ^{-/-} input DNA	169073268

Table S3. Published high-throughput ChIP-Seq data summary (related to Figure 3)

ChIP Samples	GEO Accession	Publications
Lsd1 R1	GSM687281	Whyte 2012(Whyte et al., 2012)
Lsd1 R2	GSM687282	Whyte 2012
Med12 R1	GSM560344	Kagey 2010 (Kagey et al., 2010)
Med12 R2	GSM560345	Kagey 2010
Med1 R1	GSM560347	Kagey 2010
Med1 R2	GSM560348	Kagey 2010
Smc1 R1	GSM560341	Kagey 2010
Smc1 R2	GSM560342	Kagey 2010
Smc3 R1	GSM560343	Kagey 2010
Smc3 R2	GSM560344	Kagey 2010
H3K79me2 R1	GSM307150	Marson 2008 (Marson et al., 2008)
H3K79me2 R2	GSM307151	Marson 2008
H3K36me3 R1	GSM307152	Marson 2008
H3K36me3 R2	GSM307153	Marson 2008
Nanog R1	GSM307140	Marson 2008
Nanog R2	GSM307141	Marson 2008
Pou5f1/Oct4	GSM307137	Marson 2008
Sox2 R1	GSM307138	Marson 2008
Sox2 R2	GSM307139	Marson 2008
Input DNA	GSM307155	Marson 2008
Input DNA	GSM307154	Marson 2008
Klf	GSM288354	Chen 2008(Chen et al., 2008)
Esrrb	GSM288355	Chen 2008
GFP (control)	GSM288358	Chen 2008
Suz12	GSM1199188	Kaneko 2013(Kaneko et al., 2013)
Suz12	GSM1199189	Kaneko 2013
Ezh2 2 R1	GSM1199182	Kaneko 2013
Ezh2 2 R2	GSM1199183	Kaneko 2013
Input DNA	GSM1199187	Kaneko 2013
H3K4me1	GSM723016	Shen 2012(Shen et al., 2012)
Input DNA	GSM723020	Shen 2012
Jarid2	GSM465889	Peng 2009(Peng et al., 2009)
Input DNA	GSM480164	Peng 2009
Ezh2 1	GSM480161	Peng 2009

Summary of downloaded datasets, and associated GEO Accessions and publications.

Table S4. ChIP-Seq peak identification and alignment methods (related to Figure 3)

Sample	Other Bowtie Parameters	SICER Window/Gap Size (bp)	ChIP-Seq Control
H3K4me3	-l 50 -n 2	200/200**	Our Input
H3K27me3	-l 50 -n 2	200/600**	Our Input
H3K27ac	-l 50 -n 2	200/600	Our Input
RNA Pol II	-l 50 -n 2	200/600	Our Input
Lsd1	-l 26 -n 1	200/400	Our Input
Med12	-l 26 -n 1	200/400	Our Input
Med1	-l 26 -n 1	200/400	Our Input
Smc1	-l 26 -n 1	200/400	Our Input
Smc3	-l 26 -n 1	200/400	Our Input
H3K79me2	-l 26 -n 1	200/600	Marson Input
H3K36me3	-l 26 -n 1	200/600	Marson Input
Nanog	-l 26 -n 1	200/400	Marson Input
Pou5f1/Oct4	-l 26 -n 1	200/400	Marson Input
Sox2	-l 26 -n 1	200/400	Marson Input
Klf	-l 26 -n 1	200/400	GFP ChIP
Esrrb	-l 26 -n 1	200/400	GFP ChIP
Ezh2 (Kaneko)	-l 46 -n 2	200/400	Kaneko Input
Suz12	-l 46 -n 2	200/400	Kaneko Input
H3K4me1	-l 26 -n 1	200/200	Shen Input
Jarid2	-l 45 -n 2	200/400	Peng Input
Ezh2 (Peng)	-l 26 -n 1	200/400	Peng Input

ChIP-Seq methods: The following provides information on the parameters used to align reads and SICER peak identification parameters. For bowtie, the $-l$ length parameter was chosen to be consistent with the shortest read length for the pool of reads associated with that dataset. The number of mismatches was chosen to be 1 for reads of length of about 25, and 2 for reads of length of about 50.

Table S5. RT primer sequences (related to Figure 1, 2, 3, 4 & 6)

Name of the RT primers	Sequences
PPD_Gtl2_RT_F	TTGCACATTTCTGTGGGAC
PPD_Gtl2_RT_R	AAGCACCATGAGCCACTAGG
PPD_Rian_RT_F	CGTGTGTGTGTGTGTGGT
PPD_Rian_RT_R	GCCAAGGTCTCTACCAGCAG
PPD_Mirg_RT_F	GGCAAGGTCTAGGATGGACA
PPD_Mirg_RT_R	CGCCAGCTTCTGAATACTCC
PPD_Dlk1_RT_F	GACCTGGAGAAAGGCCAGTA
PPD_Dlk1_RT_R	AGGGAGAACCATTGATCACG
PPD_Dio3_RT_F	CCCATGACACAGATGAGCAC
PPD_Dio3_RT_R	CCTGAGAGCAAGCCAAAAAC
PPD_Ezh1_RT_F	CAATAACTATGATGGCAAAGTCCAC
PPD_Ezh1_RT_R	CTCCTCCTCATCAGAGTACTGGTT
PPD_Ezh2_RT_F	GGGAGAGAACAATGATAAAGAAGAAG
PPD_Ezh2_RT_R	ATTCTCAGGAGGTTCAATATTTGG
PPD_Nanog_RT_F	AGGGTCTGCTACTGAGATGCTCTG
PPD_Nanog_RT_R	CAACCACTGGTTTTTCTGCCACCG
PPD_Pou5f1_RT_F	CTGAGGGCCAGGCAGGAGCACGAG
PPD_Pou5f1_RT_R	CTGTAGGGAGGGCTTCGGGCACTT
PPD_Dnmt1_RT_F	GGAAGGCTACCTGGCTAAAGTC
PPD_Dnmt1_RT_R	ATTTGAGTCTGCCATTTCTGCT
PPD_Dnmt3a_RT_F	GAGATGGCAAGTTCTCAGTGGT
PPD_Dnmt3a_RT_R	GAGGACTTCGTAGATGGCTTTG
PPD_Dnmt3b_RT_F	CAGGAGTACCCTGTGGAGTTTC
PPD_Dnmt3b_RT_R	ATCCTGGCTCAAGTCAACTGAT
PPD_Dnmt3L_RT_F	GATAAGTTCCTGGAGTCCCTCTT
PPD_Dnmt3L_RT_R	TGTCCACACACTCGAAACAGTAG
PPD_Dicer_RT_F	AAAGAGCTGGCCCATCAGA
PPD_Dicer_RT_R	CTGACGGCTGACACTTGTTG
PPD_Drosha_RT_F	CGGGATCGAGAGAGACACAG
PPD_Drosha_RT_R	GGCTCAGGAGCAACTGGTAA
PPD_Ago2_RT_F	CACCGGGAGAACAATCAAAC
PPD_Ago2_RT_R	ACTCTCCGAGGGCATTCTC
PPD_U1_RT_F	ATACTTACCTGGCAGGGGAG
PPD_U1_RT_R	CAGGGGGAAAGCGCGAACGCA
PPD_Gapdh_RT_F	AAATTCAACGGCACAGTCAAG
PPD_Gapdh_RT_R	CACCCCATTTGATGTTAGTGG

Table S6. miRNA RT primer sequences (related to Figure 1 & 2)

Name of the RT primers	RT primer sequences
PPD_rt_miR127_rv	CTCAACTGGTGTCTGGAGTCGGCAATTCAGTTGAG-AGCCAAGC
PPD_rt_miR127_fw	ACACTCCAGCTGGG-TCGGATCCGTCTGAGC
PPD_rt_miR134_rv	CTCAACTGGTGTCTGGAGTCGGCAATTCAGTTGAG-CCCCTCTG
PPD_rt_miR134_fw	ACACTCCAGCTGGG-TGTGACTGGTTGACCA
PPD_rt_miR323-3p_rv	CTCAACTGGTGTCTGGAGTCGGCAATTCAGTTGAG-AGAGGTTCG
PPD_rt_miR323-3p_fw	ACACTCCAGCTGGG-CACATTACACGGTCTGA
PPD_rt_miR410_rv	CTCAACTGGTGTCTGGAGTCGGCAATTCAGTTGAG-ACAGGCCA
PPD_rt_miR410_fw	ACACTCCAGCTGGG-AATATAACACAGATGG
PPD_rt_miR431_rv	CTCAACTGGTGTCTGGAGTCGGCAATTCAGTTGAG-TGCATGAC
PPD_rt_miR431_fw	ACACTCCAGCTGGG-TGTCTTGCAGGCCGTC
PPD_rt_miR433_rv	CTCAACTGGTGTCTGGAGTCGGCAATTCAGTTGAG-ACACCGAG
PPD_rt_miR433_fw	ACACTCCAGCTGGG-ATCATGATGGGCTCCT
PPD_rt_miR130a_rv	CTCAACTGGTGTCTGGAGTCGGCAATTCAGTTGAG-ATGCCCTT
PPD_rt_miR130a_fw	ACACTCCAGCTGGG-CAGTGCAATGTAAAA
PPD_rt_universal	CTCAAGTGTCTGGAGTCGGCAA

Table S7. miRNA northern probes (related to Figure 1)

miRNAs	miRNA sequences	Northern probes
miR-127	UCGGAUCCGUCUGAGCUUGGCU	AGCCAAGCTCAGACGGATCCGA
miR-134	UGUGACUGGUUGACCAGAGGGG	CCCCTCTGGTCAACCAGTCACA
miR-323-3p	CACAUUACACGGUCGACCUCU	AGAGGTTCGACCGTGTAAATGTG
miR-410	AAUAUAACACAGAUGGCCUGU	ACAGGCCATCTGTGTTATATT
miR-431	UGUCUUGCAGGCCGUAUGCA	TGCATGACGGCCTGCAAGACA
miR-433	AUCAUGAUGGGCUCCUCGGUGU	ACACCGAGGAGCCCATCATGAT
miR-130a	CAGUGCAAUGUAAAAGGGCAU	ATGCCCTTTTAACATTGCACTG
U6 snRNA	GUGCUCGCUUCGGCAGCACA	TGTGCTGCCGAAGCGAGCAC

SUPPLEMENTAL EXPERIMENTAL PROCEDURES

Small RNA sequencing (RNA-Seq) analyses

Small RNA sequencing was performed with the SOLiD platform. Reads were trimmed and aligned in colorspace. Trimming of the 3' adapter was performed with the software cutadapt using the command:

```
cutadapt --trim-primer -z -c -e 0.3 -a 330201030313112312 -m 10 -o reads.fastq reads.csfasta reads.qual
```

Reads were then aligned to mouse genome version mm9 using bowtie. Alignments were also performed in colorspace, using the command:

```
bowtie -C -S -a -k 10 -m 10 --best -l 20 -q mm9 c reads.fastq > reads.sam
```

Size selected small RNAs (18-40 nt) were sequenced from wild-type (CJ7), *Ezh2*^{-/-}, *Eed*^{-/-} and *Jarid2*^{-/-} mESCs. A summary of the libraries sequenced is given in *Table S1*.

RNA sequencing (RNA-Seq) analyses

RNA was sequenced with the Illumina pipeline, aligned to mm9 and mm10 genome using TopHat v2.0.9. Differential expression was determined using Cuffdiff v2.2.1 and the GRCm38 (mm10) Ensembl genome annotation downloaded from the UCSC Genome Bioinformatics website “Tables” tool. Alignments were made with `--no-novel-juncs` and `--no-coverage-search`. Please see *Table S2* for data summary.

Co-Immunoprecipitation (Co-IP) and Western blot

For each IP, cells were harvested from a 15 cm dish, and washed twice with ice cold PBS. Cell pellet was allowed to swell in twice the volume of hypotonic solution (10 mM HEPES- pH 7.3, 1.5 mM MgCl₂, 10 mM KCl, 1 mM DTT, 1 mM PMSF and protease inhibitors), and passed through a 26^{1/2}-gauge needle 5 times, followed by centrifugation at 14,000 rpm for 20-30 seconds. The cloudy supernatant cytoplasmic fraction was removed, and then the cell pellet was resuspended in the same volume of high salt buffer (20 mM HEPES-pH 7.3, 1.5 mM MgCl₂, 420 mM KCl, 0.2 mM EDTA, 30% Glycerol, 1 mM DTT, 1 mM PMSF and protease inhibitors) and rotated for 1-2 hour at 4°C. Then, neutralizing buffer “without salt” (20 mM HEPES-pH 7.3, 0.2 mM EDTA, 20% Glycerol, 1 mM DTT, 1 mM PMSF and protease inhibitors) was added to the nuclear extract (NE) to bring the salt concentration to around 150 mM. NE was centrifuged at 14,000 rpm for 20 min at 4°C, and the supernatant was collected. The volume of supernatant was increased to 1ml with IP buffer (combining high salt buffer and neutralizing buffer to make a final concentration of 150 mM, with 1 mM DTT, 1 mM PMSF and protease inhibitors). The supernatant was pre-cleared with either Protein-A or G agarose beads (Roche). The 5%-10% of cleared supernatant was collected as an input, and rest of the supernatant was incubated with antibody overnight at 4°C. The next day either Protein-A or G agarose beads were added to it (depending upon the antibody), and incubated for 2-3 hours at 4°C to IP endogenous protein against the specific antibody used. Subsequently, IP-ed protein-beads were washed 3 times with IP buffer, each for 5 minutes at 4°C. IP-ed proteins and their interacting partners were eluted from beads in

XT buffer (Bio-Rad) by heating at 95°C for 10 minutes, and resolved on a 4-12% gradient Bis-Tris gel (Bio-Rad) and analyzed by western blot using specific antibodies.

Antibodies

Ezh2 (D2C9 XP: 5246S, Cell signaling) (AC22: 3147, Cell signaling) (ChIPAb+ Ezh2, clone AC22 (17-662), Millipore); Suz12 (P-15: sc-46264, Santa Cruz); Jarid2 (NB100-2214, Novus Biologicals); H3K4me3 (ab1012, Abcam); H3K9me3 (ab8898, Abcam); H3K27me3 (ab6002, Abcam); H3K27ac (ab4729, Abcam); RNA Pol II 8WG16 (MMS-126R, Covance); Actin (Clone C4: MAB1501R, Millipore); Dnmt1 (39204, Active motif); Dnmt3a (IMG-268A, Imgenex) (ab13888, abcam) (ab2850, abcam); Dnmt3b (IMG-184A, Imgenex) (ab122932, abcam); Dnmt3l (IMG-6809A, Imgenex) (12309, Cell signaling).

Chromatin immunoprecipitation (ChIP)

ChIP was performed as described previously with some modifications (Das et al., 2014). Input genomic DNA was used for the reference sample. Briefly, cells were crosslinked directly on 15 cm dishes with 37% formaldehyde solution (Calbiochem) to a final concentration of 1% for 8 min at room temperature with gentle shaking. The reaction was quenched by adding 2.5M glycine to a final concentration of 0.125 M. Cells were washed twice with PBS, trypsinized and washed twice with PBS. Cell pellet was resuspended in SDS-ChIP buffer (20 mM Tris-HCl pH 8.0, 150mM NaCl, 2 mM EDTA, 0.1% SDS, 1% Triton X-100 and protease inhibitor), and chromatin was sonicated to around 200-500 bp. Sonicated chromatin were pre-cleared with either Protein-A or Protein-G agarose (Roche)

beads. Cleared samples were incubated with 5-10 μg antibody overnight at 4°C. After overnight incubation, protein A or G agarose beads were added to the ChIP reactions and incubated for 2-3 hours at 4°C to IP chromatin. Subsequently, beads were washed twice with 1 ml of low salt wash buffer (50 mM HEPES pH 7.5, 150 mM NaCl, 1 mM EDTA, 1% Triton X-100, 0.1% sodium deoxycholate), once with 1 ml of high salt wash buffer (50 mM HEPES pH 7.5, 500 mM NaCl, 1 mM EDTA, 1% Triton X-100, 0.1% sodium deoxycholate), once with 1 ml of LiCl wash buffer (10 mM Tris-HCl pH 8.0, 1 mM EDTA, 0.5% sodium deoxycholate, 0.5% NP-40, 250 mM LiCl), and twice with 1 ml of TE buffer (10 mM Tris-HCl pH 8.0, 1 mM EDTA, pH 8.0). The chromatin was eluted and reverse-crosslinked at 65°C overnight in SDS elution buffer (300 μl) (1% SDS, 10 mM EDTA, 50 mM Tris-HCl, pH 8.0). The next day, an equal volume of TE was added (300 μl). ChIP DNA was treated with 1 μl of RNaseA (10 mg/ml) for 1 hour, and with 3 μl of proteinase K (20 mg/ml) for 3 hours at 37°C, and purified using phenol-chloroform extraction, followed by QIAquick PCR purification spin columns (Qiagen). Finally, ChIP-DNA was eluted from the column with 40 μl of water. For several factors we used multiple individual ChIPs. At the end, all eluted ChIP-DNA samples were pooled and precipitated to enrich the ChIP-DNA material to make libraries for sequencing. Input ChIP samples were reserved after the pre-clear step and continued from reverse cross-linking step until the end, same as other ChIP samples. All ChIP primers are listed here.

ChIP primer sequences:

Primer names	Sequences
PPD_IGDMR_a_F	ACCCACCAGAGCAGAATTT
PPD_IGDMR_a_R	GCAGGTCAGCACTTCCTCAT
PPD_IGDMR_b_F	CCTTCTACGTAAAAAGTGCTACGA
PPD_IGDMR_b_R	CTGTA ACTATGGTGACTTGTGCATC
PPD_IGDMR_c_F	CCTTGCGCACAGATACTTGA
PPD_IGDMR_c_R	GCTGTAAACGGACCGTGTGTA
PPD_IGDMR_d_F	GCTCAGGTTCAAGTCGGCTA
PPD_IGDMR_d_R	TACTGCTCTGTGCCGTGAAG
PPD_IGDMR_e_F	CAAGTCAACAGGCCTACTCTGTAGT
PPD_IGDMR_e_R	CATATACCGTGAATTGCAGTGAGTA
PPD_IGDMR_f_F	GCTATGCTGTTTCTTTCTTTTCCTT
PPD_IGDMR_f_R	ATCCCAATCTGTGAGAATGTTTTA
PPD_IGDMR_g_F	AATGGGATCACGCGAGTAAG
PPD_IGDMR_g_R	GCTCCATGCTATTGGAGGTC
PPD_IGDMR_h_F	GCTTTGGAATTCCTGATGGA
PPD_IGDMR_h_R	TCAGCTCACAAACTGCCATT
Nanog_0.2up_F	AATGAGGTAAAGCCTCTTTTTGG
Nanog_0.2up_R	ACCATGGACATTGTAATGCAAA
Klf4_2_F	GTGCGAGTGCCTAGCTTGTA
Klf4_2_R	AAGGAAGGCGTTCCAGATTT

ChIP library generation and sequencing

Purified ChIP DNA was measured in Qubit (Invitrogen). 2-10 ng of purified ChIP DNA was used to prepare sequencing libraries, using NEB next generation ChIP sequencing Kit (NEB) and Illumina ChIP seq kit (Illumina) according to the manufacture's instructions. All libraries were checked through a Bio-analyzer for quality control purposes. ChIP sequencing was performed using Illumina Hiseq 2000. Raw data were processed through Illumina software pipeline.

ChIP sequencing (ChIP-Seq) analyses

All ChIP-seq samples were aligned with Bowtie v0.12.9 to the mm9 genome index with the following parameters: -S -m 1 -a -best -q. Custom options are found in the *Table S5*. Significant peaks were identified with SICER v1.1, and the following parameters: FDR 0.05, redundancy threshold: 1, fragment size: 150, species: mm9, effective genome size: .79 for samples with aligned read length of 46 or 50, .70 for those with aligned read length of 26 (Koehler et al., 2011). Window sizes for SICER were 200, and gap sizes were chosen as per recommendations in associated publication (Zang et al., 2009) to be 200 for H3K4me3, 600 for H3K27me3, and similarly for other chromatin marks. For transcription factors and sharply peaked binding proteins we used a gap length of 400. All ChIP-Seq data used for this study are summarized in *Table S3* and *S4*.

Genomic deletion using the CRISPR/Cas9 nuclease system

CRISPR design and creation:

Single-guide RNA (sgRNA)-specifying oligo sequences were chosen to minimize likelihood of off-target cleavage based on publicly available online tools. “CACC” was added to the 5’ end of the sgRNA-specifying oligo sequence and “AAAC” was added to the 5’ end of the reverse complement of the sgRNA-specifying oligo for cloning using the BbsI restriction enzyme. G was added immediately following CACC if the first nucleotide was A, T, or C (in these cases C was added at the 3’ end of the reverse complement oligo). The two oligos were phosphorylated and annealed using the following conditions: guide sequence oligo (10 μ M), guide sequence reverse complement

oligo (10 μ M), T4 ligation buffer (1X) (New England Biolabs), and T4 polynucleotide kinase (5U) (NEB) with the following temperature conditions: 37°C for 30 minutes; 95°C for 5 minutes and then ramp down to 25°C at 5°C/minute. The annealed oligos were cloned into pSpCas9(BB) (pX330; Addgene plasmid ID: 42230) using a “Golden Gate Assembly” strategy with the following conditions: 100 ng of circular pX330 vector, annealed oligos (0.2 μ M), NEB 2.1 buffer (1X) (NEB), BbsI restriction enzyme (20 U) (NEB), ATP (0.2 mM) (NEB), BSA (1X) (NEB), and T4 DNA ligase (750 U) (NEB) with the cycling conditions of 20 cycles of 37°C for 5 minutes, 20°C for 5 minutes; 80°C for 20 minutes.

Single-guide RNA (sgRNA) oligos for CRISPRs:

Primer names	Sequences
PPD_IGDMR/Enh1_5end-F	caccgCTAATAAAGAGTAGGCGAGC
PPD_IGDMR/Enh1_5end-R	aaacGCTCGCCTACTCTTTATTAGc
PPD_IGDMR/Enh1_3end-F	caccGTGTTGAACGTATGGCCACG
PPD_IGDMR/Enh1_3end-R	aaacCGTGGCCATACGTTCAACAC
PPD_Enh2_5end-F	caccgAGGAGATGGAATCAGCGGGT
PPD_Enh2_5end-R	aaacACCCGCTGATTCCATCTCCTc
PPD_Enh2_3end-F	caccGCTCCGTGCAAAAGGTCGCC
PPD_Enh2_3end-R	aaacGGCGACCTTTTGCACGGAGC
PPD_Non-Enh2_5end-F	caccGGAGACAGACTACAGCCGGT
PPD_Non-Enh2_5end-R	aaacACCGGCTGTAGTCTGTCTCC
PPD_Non-Enh2_3end-F	caccgTGAGCGGCGGTCCGTCCTACT
PPD_Non-Enh2_3end-R	aaacAGTGGACGGACCGCCGCTCAc
PPD_Dlk1 prom_5end-F	caccGAGTGATACATTTATTGGGCC
PPD_Dlk1 prom_5end-R	aaacGGCCCAATAAATGTATCACTC
PPD_Dlk1 prom_3end-F	caccGCAGCCTCGCAGAATCCATAC
PPD_Dlk1 prom_3end-R	aaacGTATGGATTCTGCGAGGCTGC
PPD_Gtl2 prom_5end-F	caccGAAATAAGGATGGGGTAACGG
PPD_Gtl2 prom_5end-R	aaacCCGTTACCCCATCCTTATTTC
PPD_Gtl2 prom_3end-F	caccGTCGCCAAGCGTTTCCGAC
PPD_Gtl2 prom_3end-R	aaacGTCGAAACCGCTTGGCGAC

Screening for biallelic deletion clones: Mouse ES cells (mESCs) were cultured as described above. $1-2 \times 10^6$ cells were electroporated with 1 μg pmaxGFP plasmid (Lonza), and 2 μg of each pX330-guide RNA plasmid using the ECM 830 Square Wave Electroporation System (Harvard Apparatus). Specifically, cells were resuspended in 100 μl of mouse electroporation buffer (Lonza), and electroporated at 250 V for 5 ms, in 2 mm cuvettes (Harvard Apparatus). 500 μl of mESCs medium was immediately added to the cells after electroporation, and mESCs were plated on irradiated mouse fibroblasts.

The highest 3-5% GFP⁺ cells were sorted using a FACS Aria cell sorter (BD Biosciences) 2-3 days post-electroporation. Approximately 15,000 GFP⁺ mESCs were plated on 10 cm irradiated mouse fibroblasts to obtain single cell-derived clones. After 7-10 days, single clones were picked and transferred to a 96-well plate. Individual clones were then screened for CRISPR-mediated biallelic deletion. Genomic DNA (gDNA) was extracted using 50 μL QuickExtract DNA Extraction Solution per well (Epicentre) for 65°C, 6 minutes and 98°C, 2 minutes. Polymerase chain reaction (PCR) was performed using two sets of primers (deletion and non-deletion primer pair): one set to amplify a sequence overlapping the segment to be deleted (“non-deletion band”) and another set that only amplify in the presence of a deletion (“deletion band”) using the Qiagen HotStarTaq 2x master mix (Qiagen), following cycling conditions: 95°C for 15 minutes; 35 cycles of 95°C for 15 seconds, 60°C for 1 minute, 72°C for 1 minute; 72°C for 10 minutes. Mono-allelic deletion clones were defined as having PCR amplification of both the non-deletion band and deletion band. Biallelic deletion clones were defined as having PCR amplification of the deletion band and absence of the non-deletion band. Deletion and non-deletion amplicons from non-deletion, mono-allelic, and biallelic deletion clones

were subjected to Sanger sequencing. All deletion and non-deletion primer pairs are listed here.

Primer pair used to screen CRISPR mediated biallelic deletion clones:

Deleted genomic regions	Primer pair for deletion screen	Primer names	Sequences
IG-DMR	Deletion primer pair	IGDMR/Enh1_DEL_F IGDMR/Enh1_DEL_R	GTCAATCTGAAAAGTGGCAAAAA TTCCAGAAAAGTGGTCTGTTT
	Non-deletion primer pair	IGDMR/Enh1_5flank_F IGDMR/Enh1_5flank_R	GTCAATCTGAAAAGTGGCAAAAA GGGAGGGAGAGAAGGAGAACTA
Enh2	Deletion primer pair	Enh2_DEL_F Enh2_DEL_R	CTCAGATGCTGTTTCTCACCTCT TATCTTCCTTCACAGCCTCTCG
	Non-deletion primer pair	Enh2_5flank_F Enh2_5flank_R	ATTCCCATCTCCTTGTCTTCC TCCTCAAGCACTGCATAAACTG
Non-Enh2	Deletion primer pair	Non-Enh2_DEL_F Non-Enh2_DEL_R	TAGAATCCAACAGACCCCTGAC ACTGTTTACCCAACTGAGTCGAA
	Non-deletion primer pair	Non-Enh2_5flank_F Non-Enh2_5flank_R	AGGCAAGTGCTTTTTACCACTG TGGTGGATGTTTTCAATGACAG
Dlk1	Deletion primer pair	Dlk1_prom_DEL_F Dlk1_prom_DEL_R	CCCATTTACCAAAGGAGCTATG CTCTCTCCTGTACCCCTCCTTC
	Non-deletion primer pair	Dlk1_prom_5flank_F Dlk1_prom_5flank_R	TGTGTGAGAGAGAGAGAGAGAGAG/
Gtl2	Deletion primer pair	Gtl2_prom_Del_F Gtl2_prom_Del_R	AAGCTGACAAACACATTTAAGCA GCTGTGAAGGAAAGACAGACT
	Non-deletion primer pair	Gtl2_prom_5flank_F Gtl2_prom_3flank_F	CAGACAGAGAAAACAGATCCCATC ATCTGGAAAAAGGAAAGAGTTGG

Enhancer reporter assay

Dual-luciferase assays in mESCs were performed using the Dual-Luciferase Reporter Assay System following the manufacturer's instructions (Promega). Genomic DNA fragments containing the putative enhancers (Enh-1, Enh-2 and Nanog Enh) and control non-enhancer regions (Non-Enh1, Non-Enh2) were cloned into the pGL3-basic vector.

Constructs were transfected into mESCs cells by nucleofection, and luciferase activities were measured following standard protocols.

Primers used for cloning enhancer regions for reporter assay:

Primer names	Sequences
PPD_IGDMR/Enh1_F	ACGCGTCGACGTCGGCCATAGCGGCCGCGGAATTGGGCTCAAAGCTCCACAT
PPD_IGDMR/Enh1_R	ACGCGTCGACGTCGGCCATAGCGGCCGCGGAAAGGGGCCTCTCCAGAGCAGG
PPD_Enh2_F	ACGCGTCGACGTCGGCCATAGCGGCCGCGGAACCCTCCAGTGAGGACTCAGA
PPD_Enh2_R	ACGCGTCGACGTCGGCCATAGCGGCCGCGGAAGACATTGGACAACAAGGAGG
PPD_Nanog_Enh_F	ACGCGTCGACGTCGGCCATAGCGGCCGCGGAAGTATTATTATACTGCCTGG
PPD_Nanog_Enh_R	ACGCGTCGACGTCGGCCATAGCGGCCGCGGAAGTTGAGTTAAGTACTCGGACT
PPD_Non-Enh1_F	ACGCGTCGACGTCGGCCATAGCGGCCGCGGAAAGCTGATGGGCCTTACAAAG
PPD_Non-Enh1_R	ACGCGTCGACGTCGGCCATAGCGGCCGCGGAATTGGTTGATACGAAGATGTG
PPD_Non-Enh2_F	ACGCGTCGACGTCGGCCATAGCGGCCGCGGAAAGGACAATAGAAAAGTAACA
PPD_Non-Enh2_R	ACGCGTCGACGTCGGCCATAGCGGCCGCGGAAAGCGGTATATAGATATAC

Chromosome Conformation Capture (3C)

3C assay was performed as described previously (Hagège et al., 2007; Xu et al., 2012) with some modifications. Briefly, mESCs were harvested and crosslinked with 2% formaldehyde for 10 min at room temperature. Crosslinked cells were lysed with ice-cold lysis buffer (10 mM Tris-HCl, pH 8.0, 10 mM NaCl, 0.2% NP-40, 1 mM dithiothreitol) for 10 min. The nuclei were harvested and resuspended in appropriate restriction enzyme buffer containing 0.3% SDS and incubated at 37°C for 1 hour with vigorous shaking. Triton X-100 was then added to 2% final concentration to sequester the SDS, and samples were incubated at 37°C for another 1 hour. Samples were digested with NheI (for IG-DMR/Enh1, *Gtl2* promoter, Enh2 and *Dio3* promoter) or ScaI (for Nanog) overnight at 37°C. DNA ligation was performed at 16°C for 4 hours and 30 min at room temperature. Crosslinks were reversed, and DNA was then purified by phenol extraction

and ethanol precipitation. To correct for the PCR amplification efficiency of different primer sets, BAC clones containing the complete mouse IG-DMR/Enh1, *Gtl2* promoter (RP23-117C15), Enh2 (RP23-409I23), *Dio3* promoter (RP24-316E16) and *Nanog* promoter (RP23-474F18) were used as control templates. Equimolar amounts of BAC DNA were mixed, digested, and ligated. Quantification of the data was performed by quantitative real-time PCR using the SYBR Green Supermix (Bio-Rad). 3C product detection was done by RT-qPCR, and the average signal was corrected by dividing the average signal in the BAC control template.

RNA immunoprecipitation (RIP)

Mouse ES Cells were grown on gelatin coated 15 cm dishes, ~10 million cells were harvested and resuspended in 2ml of 1X PBS. Nuclear Isolation Buffer (2ml) (1.28M sucrose, 40mM Tris-Cl pH 7.4, 20mM MgCl₂ and 4% Triton X-100 with freshly added 1:1000 Protease inhibitor (Sigma), 1mM DTT) and water (6ml) were added to the resuspended cells and incubated for 20-30 min on gentle rotation at 4°C. Nuclei were pelleted by centrifugation at 2500g for 15 min at 4°C. Then, nuclei pellet were resuspended in 1ml of RNA immunoprecipitation buffer (RIP buffer-150mM KCl, 25mM Tris-Cl pH 7.4, 5mM EDTA, 0.5% NP40 with freshly added 1:200 Protease inhibitor (Sigma), 1mM DTT and 200 units of RNaseOUT (Invitrogen/ Life tech)). Resuspended nuclei were divided into two fractions of 500µl each (one for mock and one for IP), and passed through 26^{1/2} G syringe 5 times. Nuclear membrane and debris were pelleted by centrifugation at 13000 rpm for 15 min at 4°C; supernatant was collected and 5µg of antibody against protein of interest (IP sample) and normal IgG (as control) (mock

sample) were added and incubated for overnight at 4°C with gentle rotation. Next day, Protein A/G Dynabeads (Invitrogen/ Life tech) (75µl) were added to this and incubated for 2 hours at 4°C with gentle rotation to capture the antibodies that bound to protein of interest. Beads were pelleted using magnetic stand, and washed twice with 1 ml of 150mM of RIP buffer, followed by 3 times wash with 1ml of 1M of RIP buffer. Immunoprecipitated protein was resuspended in 1ml of Trizol (Invitrogen) and RNAs that are bound to protein of interest were extracted according to the manufacture's instructions. RNA was eluted in 15µl of water and treated with TURBO DNA-free kit (Ambion/ Life tech) to remove the DNA contamination as per as manufacture's instructions.

DNA-free RNA was converted to cDNA using iScript cDNA synthesis kit (Bio-Rad), followed by qRT-PCR using iQ SYBR Green supermix (Bio-Rad) to detect the specific RNAs that are bound with protein of interest.

ChIPAb+ Ezh2, clone AC22 (17-662, Millipore), RIPAb+ Eed (03-196, Millipore), Suz12 (39357, Active motif) and Dnmt3a (IMG-268A, Imgenex) were used for RIP.

Gene expression microarray analyses

Affymetrix GeneChip mouse genome 430A 2.0 arrays were used for gene expression profiles. Total RNAs were extracted using RNeasy plus mini kit (Qiagen) and subsequent cDNA synthesis, labeling, hybridization, washing and scanning were performed by the Microarray Core Facility at the Dana Farber Cancer Institutes (DFCI). Expression data

were normalized using dChip software. The raw data set used in this study is available at Gene Expression Omnibus (GEO Accession: GSE58414).

Overexpression of Ezh2 and Dnmt3a

Adeno-Ezh2-GFP virus was infected in wild-type and *Dnmt3a*^{-/-} mESCs, and GFP⁺ve cells were grown after FACS sorting.

Single copy of Dnmt3a cDNA transgene was integrated at the ROSA26 locus. Dnmt3a expressed through induction of Doxycycline (unpublished). This cell line was a gift from Alex Meissner.

SUPPLEMENTAL REFERENCES

Chen, X., Xu, H., Yuan, P., Fang, F., Huss, M., Vega, V.B., Wong, E., Orlov, Y.L., Zhang, W., Jiang, J., et al. (2008). Integration of External Signaling Pathways with the Core Transcriptional Network in Embryonic Stem Cells. *Cell* *133*, 1106–1117.

Das, P.P., Shao, Z., Beyaz, S., Apostolou, E., Pinello, L., De Los Angeles, A., O'Brien, K., Atsma, J.M., Fujiwara, Y., Nguyen, M., et al. (2014). Distinct and Combinatorial Functions of Jmjd2b/Kdm4b and Jmjd2c/Kdm4c in Mouse Embryonic Stem Cell Identity. *Molecular Cell* *53*, 32–48.

Hagège, H., Klous, P., Braem, C., Splinter, E., Dekker, J., Cathala, G., de Laat, W., and Forné, T. (2007). Quantitative analysis of chromosome conformation capture assays (3C-qPCR). *Nat Protoc* *2*, 1722–1733.

Kagey, M.H., Newman, J.J., Bilodeau, S., Zhan, Y., Orlando, D.A., van Berkum, N.L., Ebmeier, C.C., Goossens, J., Rahl, P.B., Levine, S.S., et al. (2010). Mediator and cohesin connect gene expression and chromatin architecture. *Nature* *467*, 430–435.

Kaneko, S., Son, J., Shen, S.S., Reinberg, D., and Bonasio, R. (2013). PRC2 binds active promoters and contacts nascent RNAs in embryonic stem cells. *Nature Publishing Group* *20*, 1258–1264.

Koehler, R., Issac, H., Cloonan, N., and Grimmond, S.M. (2011). The uniqueome: a mappability resource for short-tag sequencing. *Bioinformatics* *27*, 272–274.

Marson, A., Levine, S.S., Cole, M.F., Frampton, G.M., Brambrink, T., Johnstone, S., Guenther, M.G., Johnston, W.K., Wernig, M., Newman, J., et al. (2008). Connecting microRNA Genes to the Core Transcriptional Regulatory Circuitry of Embryonic Stem Cells. *Cell* *134*, 521–533.

Peng, J.C., Valouev, A., Swigut, T., Zhang, J., Zhao, Y., Sidow, A., and Wysocka, J. (2009). Jarid2/Jumonji Coordinates Control of PRC2 Enzymatic Activity and Target Gene Occupancy in Pluripotent Cells. *Cell* *139*, 1290–1302.

Shen, Y., Yue, F., McCleary, D.F., Ye, Z., Edsall, L., Kuan, S., Wagner, U., Dixon, J., Lee, L., Lobanenko, V.V., et al. (2012). A map of the cis-regulatory sequences in the mouse genome. *Nature* *488*, 116–120.

Whyte, W.A., Bilodeau, S., Orlando, D.A., Hoke, H.A., Frampton, G.M., Foster, C.T., Cowley, S.M., and Young, R.A. (2012). Enhancer decommissioning by LSD1 during embryonic stem cell differentiation. *Nature* *482*, 221–225.

Xu, J., Shao, Z., Glass, K., Bauer, D.E., Pinello, L., Ben Van Handel, Hou, S., Stamatoyannopoulos, J.A., Mikkola, H.K.A., Yuan, G.-C., et al. (2012). Combinatorial Assembly of Developmental Stage-Specific Enhancers Controls Gene Expression Programs during Human Erythropoiesis. *Developmental Cell* *23*, 796–811.

Zang, C., Schones, D.E., Zeng, C., Cui, K., Zhao, K., and Peng, W. (2009). A clustering approach for identification of enriched domains from histone modification ChIP-Seq data. *Bioinformatics* 25, 1952–1958.